Mechanism of N2 Reduction Catalyzed by Fe-Nitrogenase Involves Reductive Elimination of H2

Authors: Derek F. Harris, Dmitriy A. Lukoyanov, Sudipta Shaw, Phil Compton, Monika Tokmina-Lukaszewska, Brian Bothner, Neil Kelleher, Dennis R. Dean, Brian M. Hoffman, and Lance C. Seefeldt

This document is the unedited author's version of a Submitted Work that was subsequently accepted for publication in Biochemistry, copyright © American Chemical Society after peer review. To access the final edited and published work, see https://dx.doi.org/10.1021/acs.biochem.7b01142.

Harris, Derek F, Dmitriy A Lukoyanov, Sudipta Shaw, Phil Compton, Monika Tokmina-Lukaszewska, Brian Bothner, Neil Kelleher, Dennis R Dean, Brian M Hoffman, and Lance C Seefeldt. "Mechanism of N2 Reduction Catalyzed by Fe-Nitrogenase Involves Reductive Elimination of H2." Biochemistry 57, no. 5 (February 2018): 701-710. DOI:10.1021/acs.biochem.7b01142.

Made available through Montana State University's ScholarWorks
scholarworks.montana.edu

Mechanism of N_2 Reduction Catalyzed by Fe-Nitrogenase Involves Reductive Elimination of H_2

Derek F. Harris,[†] Dmitriy A. Lukoyanov,[‡] Sudipta Shaw,[†] Phil Compton,[‡]
Monika Tokmina-Lukaszewska,[§] Brian Bothner,[§] Neil Kelleher,[‡] Dennis R. Dean,[∥]
Brian M. Hoffman,[*,‡] and Lance C. Seefeldt[*,†]

[†]Department of Chemistry and Biochemistry, Utah State University, Logan, Utah 84322, United States
[‡]Departments of Chemistry and Molecular Biosciences, Northwestern University, Evanston, Illinois 60208, United States
[§]Department of Chemistry and Biochemistry, Montana State University, Bozeman, Montana 59717, United States
[∥]Department of Biochemistry, Virginia Polytechnic Institute and State University, Blacksburg, Virginia 24061, United States

ABSTRACT: Of the three forms of nitrogenase (Mo-nitrogenase, V-nitrogenase, and Fe-nitrogenase), Fe-nitrogenase has the poorest ratio of N_2 reduction relative to H_2 evolution. Recent work on the Mo-nitrogenase has revealed that reductive elimination of two bridging Fe—H—Fe hydrides on the active site FeMo-cofactor to yield H_2 is a key feature in the N_2 reduction mechanism. The N_2 reduction mechanism for the Fe-nitrogenase active site FeFe-cofactor was unknown. Here, we have purified both component proteins of the Fe-nitrogenase system, the electron-delivery Fe protein (AnfH) plus the catalytic FeFe protein (AnfDGK), and established its mechanism of N_2 reduction. Inductively coupled plasma optical emission spectroscopy and mass spectrometry show that the FeFe protein component does not contain significant amounts of Mo or V, thus ruling out a requirement of these metals for N_2 reduction. The fully functioning Fe-nitrogenase system was found to have specific activities for N_2 reduction (1 atm) of 181 ± 5 nmol NH_3 min^{-1} mg^{-1} FeFe protein, for proton reduction (in the absence of N_2) of 1085 ± 41 nmol H_2 min^{-1} mg^{-1} FeFe protein, and for acetylene reduction (0.3 atm) of 306 ± 3 nmol C_2H_4 min^{-1} mg^{-1} FeFe protein. Under turnover conditions, N_2 reduction is inhibited by H_2 and the enzyme catalyzes the formation of HD when presented with N_2 and D_2. These observations are explained by the accumulation of four reducing equivalents as two metal-bound hydrides and two protons at the FeFe-cofactor, with activation for N_2 reduction occurring by reductive elimination of H_2.

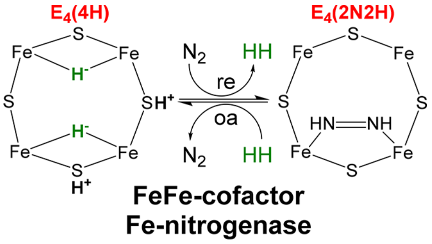

Nitrogenase is the microbial enzyme responsible for biological dinitrogen (N_2) fixation to ammonia (NH_3) and represents the largest contributor of fixed nitrogen (N) to the global biogeochemical nitrogen cycle.[1−3] There are only three known forms of nitrogenase designated as the molybdenum (Mo)-dependent, the vanadium (V)-dependent, and the iron (Fe)-dependent enzymes,[4−6] each encoded by unique gene clusters, designated *nif*, *vnf*, and *anf*, respectively.[7−9] Each nitrogenase contains a complex metal cluster called the FeMo-cofactor, FeV-cofactor, and FeFe-cofactor, as the active site for substrate reduction (Figure 1B). These multimetallic cofactors all contain Fe and S, with available evidence indicating that all three are similar, with substitution of one metal (Mo, V, or Fe).[4,5,10−13] The X-ray structure of the Mo-nitrogenase has been well established,[14] and a recent X-ray structure of the V-dependent nitrogenase confirms that the basic architectures of FeMo-cofactor and FeV-cofactor are similar, with V substituting for Mo.[15] Additionally, the structure of FeV-cofactor shows a molecule replacing one of the bridging sulfide atoms found in FeMo-cofactor. While the identity of the molecule replacing S is unknown, it has been proposed to be carbonate.[15] No structural information is available for the FeFe-cofactor in Fe-nitrogenase.

Mo-nitrogenase is the best studied of the three nitrogenase forms. It is a two-component system comprising a catalytic MoFe protein (NifDK) and electron-delivery Fe protein (NifH) (Figure 1A). The Fe protein is a homodimer that contains a single Fe_4S_4 cluster and two MgATP-binding sites.[5] The MoFe protein is a $\alpha_2\beta_2$ heterotetramer that forms two catalytic halves, with each half containing a Fe_8S_7 cluster (P-cluster) and a $MoFe_7S_9C$-homocitrate active site cofactor (FeMo-co). During catalysis, the two component proteins transiently associate, during which the Fe protein donates one electron to the MoFe protein, coupled to the hydrolysis of two MgATP. Electrons are accumulated on FeMo-cofactor, with the P-cluster proposed to act as a "deficit-spending" electron shuttle between the Fe protein and FeMo-cofactor.[5,13] Studies of the MoFe protein trapped during catalysis have shown how electrons and protons accumulate on FeMo-cofactor and how

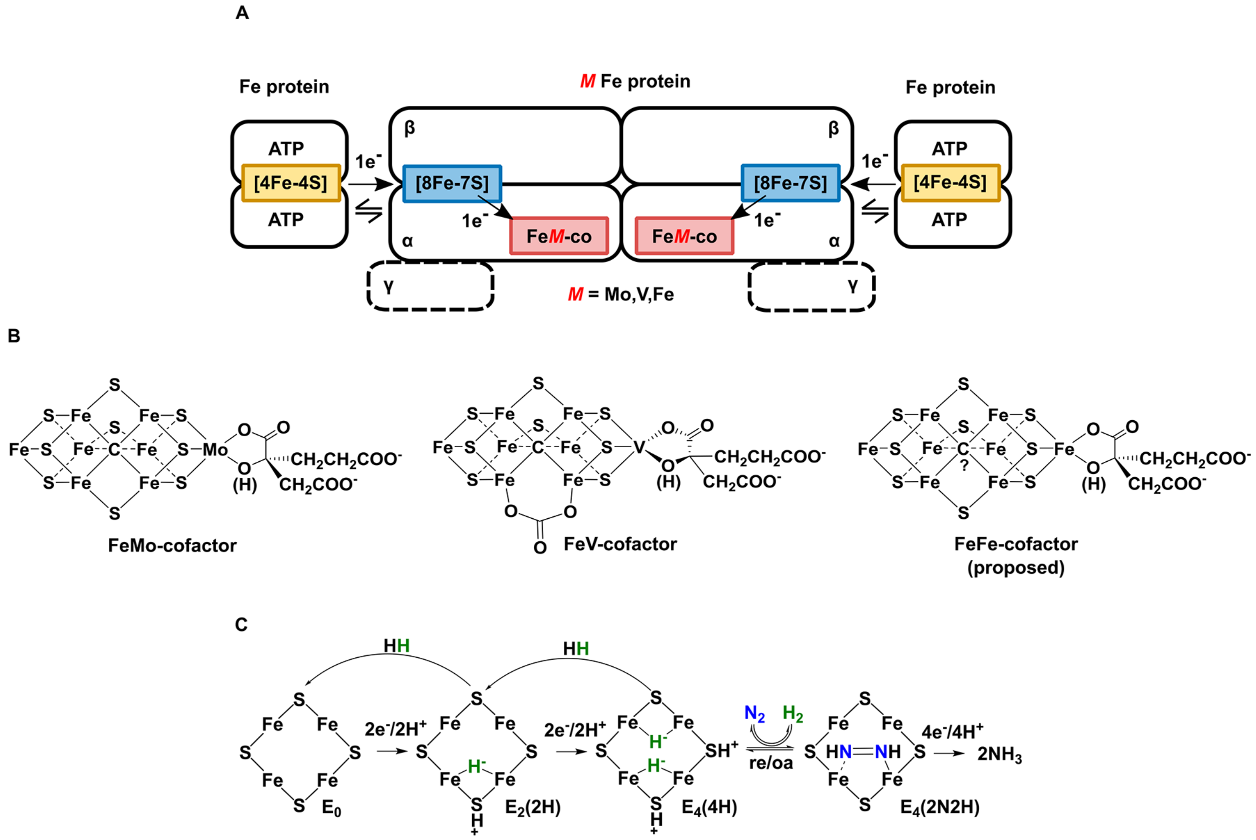

Figure 1. General nitrogenase architecture, nitrogenase cofactors, and N_2 activation mechanism. (A) Schematic of nitrogenases showing the electron delivery component (Fe protein), catalytic component (MoFe, VFe, or FeFe protein), metal clusters, and electron delivery pathway. The differing metal atom (M in red) is Mo, V, or Fe. MoFe protein is an $\alpha_2\beta_2$ heterotetramer, while VFe and FeFe proteins are $\alpha_2\beta_2\gamma_2$ heterohexamers. (B) Structural models of nitrogenase cofactors with homocitrate on the right based on crystal structures for MoFe and VFe proteins. The carbonate in the FeV-cofactor has not been unambiguously assigned. No structure for the FeFe-cofactor is available, so a model is proposed based on available data. (C) Simplified form of the N_2 activation mechanism, with cartoons of the Fe 2, 3, 6, 7 face of FeMo-cofactor in the E_0, E_2, and E_4 states (designation from the Lowe–Thorneley kinetic model) showing hydrides and protons and showing both the *re*/*oa* equilibrium with loss of H_2 and binding/reduction of N_2 (going right) and the two steps of H_2 generation by hydride protonation that occur in the absence of N_2 (going left). The exact location of the bound hydrides and protons is proposed.

the enzyme is activated for N_2 binding and reduction (Figure 1C).[13] In short, four electrons and protons must be accumulated on FeMo-cofactor to create the $E_4(4H)$ state before N_2 can be reduced. This $E_4(4H)$ state contains two Fe–H–Fe bridging hydrides. The two hydrides combine to make H_2 in a reductive elimination (*re*) reaction that is coupled to N_2 binding and reduction by two electrons/protons to the first bound intermediate, a diazenido-metal complex ($E_4(2N2H)$). The *re* step is reversible, with the oxidative addition (*oa*) of H_2 by $E_4(2N2H)$ leading to N_2 release.[13,16−19] The reversibility of this *re*/*oa* step explains early findings that two HD are formed for every D_2 consumed when nitrogenase is turned over in the presence of D_2 and N_2.[20,21] This observation can be understood from the mechanistic model as resulting from *oa* of D_2 by the $E_4(2N2H)$ state, which leads to formation of two metal-bound D^- with loss of N_2. These nonexchangeable deuterides each react with H^+ derived from solvent, yielding two HD.[20,21] Overall, the two signature features of the *re*/*oa* mechanism for N_2 activation by nitrogenase are the observations that H_2 can inhibit N_2 reduction and that turnover in the presence of N_2 and D_2 results in the formation of HD.

Studies on V-nitrogenase have indicated that while it does reduce N_2, it does so at a lower rate compared to Mo-nitrogenase, and little is known about its catalytic mechanism.[4,6,10,12,22] Even fewer studies have been conducted on Fe-nitrogenase, and less is known about its mechanism for N_2 reduction.[4,9,11,12,23−28] Like Mo-nitrogenase, Fe-nitrogenase comprises an electron-delivery Fe protein (AnfH) and catalytic "FeFe protein" (AnfDGK) (Figure 1A). Compared to the MoFe protein, the FeFe protein incorporates an extra gamma subunit per catalytic half, forming an $\alpha_2\beta_2\gamma_2$ heterohexamer (Figure 1A). Amino acid residues in the Fe protein of Mo-nitrogenase that coordinate the Fe_4S_4 cluster and nucleotide binding sites, as well as those in MoFe protein that coordinate the P-cluster and FeMo-cofactor, are conserved in the Fe-nitrogenase proteins.[8,9,29,30] Spectroscopic studies predict that Fe-nitrogenase contains a metallocluster called FeFe-co that is structurally homologous to FeMo-co of Mo-nitrogenase.[11]

While structurally and functionally similar, some aspects of catalysis by the three nitrogenases are not identical. In the case of Mo-nitrogenase, the *re*/*oa* equilibrium incorporates a mechanistically required limiting stoichiometry (eq 1) for N_2 reduction

$$N_2 + 8H^+ + 16MgATP + 8e^- \rightarrow 2NH_3 + H_2 + 16MgADP + 16P_i \quad (1)$$

as proposed by Lowe and Thorneley.[31] This limiting stoichiometry is, in fact, approached under high N_2 pressures.[32]

In contrast, under 1 atm partial pressure of N_2 (P_{N_2}), the optimal stoichiometry for Fe-nitrogenase is about 9 H_2 per N_2 reduced.[9] The mechanism-determined ratio of H_2 formed per N_2 reduced for V-nitrogenase is not known, but the observed H_2 produced/N_2 reduced ratio is between the values for the Mo- and Fe-enzymes. Overall, there is no experimental evidence to establish that the V- and Fe-nitrogenases follow the same *re*/*oa* mechanism for N_2 activation and the same mechanistic stoichiometry proposed for N_2 activation by the Mo-enzyme. Indeed, the absence of Mo in the Fe-enzyme directly raises the possibility that this enzyme could follow a different mechanism for N_2 reduction.

Here, we have purified both component proteins for the *Azotobacter vinelandii* Fe-nitrogenase and carried out experiments that reveal that this nitrogenase indeed follows the *re*/*oa* mechanism established for Mo-nitrogenase, with its "eight-electron" stoichiometry (eq 1).

■ MATERIALS AND METHODS

Reagents and General Procedures. All reagents were obtained from Sigma-Aldrich (St. Louis, MO) or Fisher Scientific (Fair Lawn, NJ) unless specified otherwise and used without further purification. Argon, dinitrogen, dihydrogen, D_2, acetylene, and ethylene gases were purchased from Air Liquide America Specialty Gases LLC (Plumsteadville, PA). Manipulation of proteins and buffers was done anaerobically in septum-sealed serum vials or flasks under an argon atmosphere or on a Schlenk line. Gas transfers were made using gastight syringes.

Strain Construction, Bacterial Growth, and Protein Expression and Purification. *A. vinelandii* strain DJ1255 was constructed in two steps. First, the tungsten-tolerant phenotype was transferred to DJ33, which is deleted for the *nifDK* genes,[33] by using chromosomal DNA isolated from CA11.6.[24] This strain is designated DJ1254 and is inactivated for the Mo-dependent system but has both the V-dependent and Fe-only nitrogen fixation systems intact. Subsequently, the V-dependent system from DJ1254 was inactivated by transformation using pDB1087 DNA that carries a kanamycin-resistance gene cartridge located within the N-terminal coding region of *vnfK*. This strain, DJ1255, is inactivated for both the Mo-dependent and V-dependent nitrogenases but retains an intact Fe-dependent nitrogenase.

Fe-nitrogenase proteins, FeFe protein (AnfDGK) and Fe protein (AnfH), were expressed in *A. vinelandii* strain DJ1255 cells grown under N_2 fixing conditions at 30 °C in Burk N-free medium[34] with Na_2MoO_4 omitted in a custom-built 100 L fermenter with stirring and aeration to an OD_{600} of 1.8−2.0 and then harvested. Mo-nitrogenase proteins were expressed in *A. vinelandii* strains DJ995 (MoFe protein, NifDK) and DJ884 (Fe protein, NifH) and grown as previously described.[35] For Mo-nitrogenase proteins, crude cell extracts were prepared and proteins were purified according to previously described methods with minor modifications.[35−37] For Fe-nitrogenase proteins, cell extracts were prepared using a French pressure cell (SLM Aminco FA-078, Aminco, Rochester, NY) operated at 1500 lb/in^2 in a degassed 50 mM Tris·HCl buffer (pH 8.0) with 2 mM sodium dithionite. All steps were conducted with oxygen-free buffers under Ar gas. This is the base buffer used throughout the purification with varying concentrations of NaCl as indicated. The cell extract was centrifuged at 50 000*g* for 1 h to remove cell debris. Lysate was then loaded onto a ∼170 mL Q-Sepharose column that had been previously washed in buffer containing 1 M NaCl and then rinsed and equilibrated in no salt buffer. The column was then washed for 2 column volumes (CV) with 10% NaCl. Proteins were separated with a NaCl gradient (20−45% NaCl over 6 CV at 5 mL/min). AnfH eluted off the column as a dark brown fraction at 24−27% NaCl, and AnfDGK eluted as a dark brown fraction at 29−35% NaCl. AnfH and AnfDGK fractions were then further purified with Sephacryl S-200 or Sephacryl S-300 columns, respectively, in buffer with 250 mM NaCl. Pooled fractions of AnfH or AnfDGK were concentrated using an Amicon (EMD Millipore, Billerica, MA) concentrator with a 60 or 100 kDa cutoff membrane, respectively, and stored in liquid nitrogen. Protein concentrations were determined by the Biuret assay using BSA as a standard. Protein purity of >85% was confirmed by sodium dodecyl sulfate polyacrylamide gel electrophoresis (SDS-PAGE) analysis using Coomassie blue staining.

Protein Identification. Protein identification from gel bands and solution digestion was performed according to standard protocols recommended by the manufacturers using a trypsin (Promega, Madison, WI) protease/complex ratio of 1:50 overnight at 37 °C (in-gel digestion) and 1:100 for 3 h at 37 °C (in-solution digestion). Proteins were identified as described[38] using a maXis Impact UHR-QTOF instrument (Bruker Daltonics, Billerica, MA) interfaced with a Dionex 3000 nano-uHPLC (Thermo-Fisher, Waltham, MA) followed by data analysis in Peptide Shaker.[39] Protein homology models were generated by Phyre2.[40]

Dinitrogen, Acetylene, Proton Reduction, and H_2 Inhibition of N_2 Assays. Substrate reduction assays were conducted in 9.4 mL serum vials containing an assay buffer consisting of a MgATP regeneration system (6.7 mM $MgCl_2$, 30 mM phosphocreatine, 5 mM ATP, 0.2 mg/mL creatine phosphokinase, 1.2 mg/mL BSA) and 10 mM sodium dithionite in 100 mM MOPS buffer at pH 7.0. After solutions were made anaerobic, headspace gases in the reaction vials were adjusted to desired partial pressures of relevant gaseous substrates or inhibitors (N_2, C_2H_2, or H_2) per condition indicated. Any remaining headspace was filled by argon. The FeFe or MoFe protein was then added to the vials, the vials were ventilated to atmospheric pressure, and the reactions were initiated by addition of the relevant Fe protein. FeFe and MoFe proteins were used at a 0.1 mg/mL concentration. Fe proteins were used at a saturating concentration of 30:1 molar ratio of Fe/FeFe and 20:1 molar ration of Fe/MoFe. Reactions were conducted at 30 °C for 8 min and then quenched by the addition of 300 μL of 400 mM EDTA (pH 8.0). The products (NH_3, H_2, and C_2H_4) from different substrate reduction assays were quantified according to published methods with minor modifications.[41,42]

Metal Content Analysis. Molybdenum and iron concentrations were determined at the Utah State University Analytics Lab on a Thermo Fisher Scientific (Waltham, MA) iCAP 6300 ICP-OES (minimum detection limit, 0.0001 μg/mL; minimum reporting limit, 0.001 μg/mL). Vanadium concentrations were determined at the Utah Veterinary Diagnostic Laboratory (UVDL, Logan, UT) using a validated protocol with argon plasma mass spectrometry (minimum detection limit, 0.0001 μg/mL; minimum reporting limit, 0.001 μg/mL). To quantify the vanadium content, analyses were performed using nitric acid digested samples. The samples were digested (1:1) in trace mineral grade nitric acid (Fisher Scientific, Pittsburgh, PA) in sealed 10 mL Oak Ridge screw-cap Teflon digestion tubes

(Nalge Nunc International, Rochester, NY) on a heat block for 2 h at 90 °C. The digests were diluted 1:10 with 18.2 mOhm water in a 15 mL polypropylene trace metal free tube. This provided a 5% nitric acid matrix for analysis, which was matrix matched for all standard curve and quality control samples. Vanadium analysis was performed using an ELAN 6000 inductively coupled plasma mass spectrometer (ICP-MS) (PerkinElmer, Shelton, CT). Five-point standard curves (0.010, 0.050, 0.100, 0.250, and 0.500 μg/mL) and quality control (QC) samples were analyzed every five samples. QC analyses were considered acceptable at ±10% of the known vanadium concentration, but they were generally less than ±5%.

HD Production. Turnover samples were prepared, initiated, and terminated as described above. Paired no-turnover control samples with both proteins excluded and the liquid volume contribution from the proteins substituted with EDTA were prepared and handled identically to the turnover samples. The ratio of the partial pressures of N_2 and D_2 in the headspaces of a sample pair was varied as desired, with Ar filling the remaining headspace. In turnover samples, FeFe and Fe proteins were each used at a 0.4 mg/mL concentration for a Fe/FeFe molar ratio of 4:1. MoFe and Fe proteins were each used at a 0.2 mg/mL concentration for a Fe/MoFe molar ratio of 4:1.

The headspace volumes of all samples were tested with an Inficon L100 RGA for the presence of H_2 and HD produced during reaction. In these experiments, a 300 μm i.d. fused silica capillary connected to the vacuum chamber on which the RGA was mounted was passed into the sample vial through a hollow needle, which had punctured the septum of the vial. Current measurements were acquired for $m/z = 2$ and 3, averaged over ∼1 min for each vial; typical measurement traces are presented in Figure S1. For each gas mixture, multiple samples were each subjected to multiples of such independent measurements. The differences in paired turnover and no-turnover samples were converted into volume units of H_2 and HD (at 1 atm, 295 K) from a calibration obtained with a set of appropriately prepared standards containing a known H_2 gas volume, which was varied from 10 to 60 μL. Comparison of paired turnover and no-turnover samples allowed us to take into account an $m/z = 2$ background, formed from H_2O and D_2 and present in all vials, which varied with the tested N_2/D_2 mixture, as well as an $m/z = 3$ background caused by contamination of the D_2 gas with HD. Measurements of $m/z = 3$ and 4 signals in no-turnover samples indicate the HD contamination as 0.15 ± 0.02%.

Statistical Analysis. Statistical significance tests (Student's *t* test) were run for the variations of H_2 and HD production as a function of the ratio of partial pressures of N_2/D_2 (Figure 7, upper and lower), using the online "*t* test" calculator https://www.graphpad.com/quickcalcs/ttest2/. Results are reported below in terms of the output *P* value, which varies between 0 and 1, and is the probability of observing a difference in the average values of two sets of measurements as large as observed in experiment, even if the two population means are identical.

Data obtained for H_2 production (upper plot of Figure 7) reveal *P* values ranging from 0.08 to 0.79 for the first four N_2/D_2 ratios, indicating that differences in the measured H_2 production during FeFe-protein turnovers at N_2/D_2 ratios of 0.1/0.9, 0.3/0.7, 0.5/0.5, and 0.7/0.3 are not statistically significant. For the highest ratio, $N_2/D_2 = 0.9/0.1$, the value of *P* ranges between 0.0011 and 0.047 in comparison with the four lower ratios, which implies that the decrease in the H_2 production induced by high pressure of N_2 during FeFe-protein turnover can be considered statistically significant or even very significant. The same statistical significance test applied to HD production (lower plot of Figure 7) gave *P* values of 0.0011 or less when comparing the two ratios with the highest HD production measured at $N_2/D_2 = 0.5/0.5$ and 0.7/0.3, with production at both lower and higher extremes of the N_2/D_2 ratio, indicating the decreases in HD production at low and high N_2/D_2 ratios are very or even extremely statistically significant.

RESULTS

Fe-Nitrogenase Properties. Both Fe-nitrogenase component proteins were expressed in a strain of *A. vinelandii* (DJ1255) that contains deletions in the Mo-nitrogenase structural genes (*nifDK*) and the V-nitrogenase structural genes (*vnfDGK*), thus precluding the presence of those other nitrogenases. AnfH (Fe protein) and AnfDGK (FeFe protein) were purified using a combination of ion exchange and size exclusion chromatography to near homogeneity, as judged by the migration on SDS-PAGE with Coomassie blue staining (Figure S2). The AnfH protein appeared as one protein on SDS-PAGE at the expected molecular weight (not shown). The AnfDGK protein appeared as three proteins, corresponding in mass to the expected subunits, with approximate 1:1:1 stoichiometry from densitometry of the Coomassie stained gel (Figure S2). The identity of all component proteins (AnfHDGK) was established by performing a trypsin digest on SDS gel fragments and analyzing the peptide fragments by mass spectrometry. Proteins were identified with 100% confidence based on 88, 76, and 23 proteolytic peptides providing 76, 66, and 65% sequence coverage for AnfK, AnfD, and AnfG, respectively. AnfH was identified with 100% confidence based on 58 proteolytic fragments providing 63% sequence coverage[43] (Figure S3). The minor protein below 48 kDa was identified as NifS.

The purified FeFe protein was subjected to inductively coupled optical emission and mass spectrometry to establish the metal content. Mo and V content were at or below the detection limits for the measurement (1 ppb), indicating a maximum possible Mo content of 0.07 mol Mo/mol protein and V content of 0.005 mol V/mol protein. Fe content was found to be 27.8 ± 0.9 mol Fe/mol protein. The predicted Fe content is 16 Fe from two P clusters and 16 Fe from the two FeFe-cofactors for a total of 32 mol Fe per mol protein. The measured Fe content is 87% of the predicted value and is consistent with occupancies in prior studies.[9] The very low upper limits to the Mo and V content confirm that the measured substrate reduction activities are not associated with these elements.

Substrate Reduction and Inhibition. The purified Fe protein (AnfH) and FeFe protein (AnfDGK) were tested for reduction of H^+, C_2H_2, and N_2 in an assay with MgATP, creatine phosphate, and creatine phosphokinase as an ATP regenerating system. Activity was only detectable in the presence of both component proteins and MgATP. Optimal activity was seen at pH 7.0, with lower activity seen above pH 7.3. Sodium dithionite ($Na_2S_2O_4$) concentrations above 2 mM did not increase activity, showing that the reactions are saturated for this reductant. Concentrations above 6 mM did not inhibit activity as has been previously reported for the FeFe protein purified from *Rhodobacter capsulatas*.[9] The specific activity was dependent on the electron flux as determined by the molar ratio Fe protein/FeFe protein, with activity

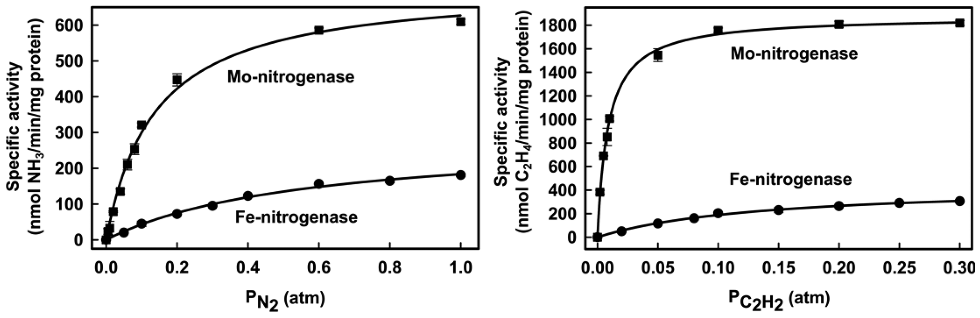

Figure 2. Specific activities for substrate reduction by Mo- and Fe-nitrogenases. Shown are the N_2 partial pressure dependence of NH_3 formation (left) and C_2H_2 on C_2H_4 formation (right) in Fe-nitrogenase (●) and Mo-nitrogenase (■). N_2 and C_2H_2 apparent K_m and V_{max} values were determined by a fit of the data to the Michaelis−Menten equation (lines). Mo-nitrogenase: apparent K_m N_2 = 0.13 ± 0.03 atm, V_{max} = 713 ± 19 nmol NH_3 min^{-1} mg^{-1} MoFe protein, and apparent K_m C_2H_2 = 0.009 ± 0.0005 atm, V_{max} = 1876 ± 20 nmol C_2H_4 min^{-1} mg^{-1} MoFe protein. Fe-nitrogenase: apparent K_m N_2 = 0.56 ± 0.06 atm, V_{max} = 286 ± 15 nmol NH_3 min^{-1} mg^{-1} FeFe protein, and apparent K_m C_2H_2 = 0.14 ± 0.01 atm, V_{max} = 450 ± 18 nmol C_2H_4 min^{-1} mg^{-1} FeFe protein. Data are the average of two independent experiments with error bars. Assays were performed as described in Materials and Methods.

Table 1. Specific Activities and Total Electron Flux in Mo- and Fe-Nitrogenase

	substrate							
enzyme	H^+		N_2[a]			C_2H_2[b]		
	H_2 specific activity	total e^-	H_2 specific activity	NH_3 specific activity	total e^-[c]	H_2 specific activity	C_2H_4 specific activity	total e^-[d]
nitrogenase	nmol/min/mg	nmol/min/mg	nmol/min/mg	nmol/min/mg	nmol/min/mg	nmol/min/mg	nmol/min/mg	nmol/min/mg
Mo	2226 ± 35	4452 ± 69	600 ± 4	605 ± 9	3016 ± 36	ND[e]	1819 ± 20	3639 ± 43
Fe	1085 ± 41	2170 ± 83	599 ± 57	181 ± 5	1739 ± 128	484 ± 3	306 ± 3	1580 ± 13

[a] 1 atm N_2. [b] 0.3 atm C_2H_2. [c] Total e^- is 2× nmol H_2 + 3× nmol NH_3. [d] Total e^- is 2× nmol H_2 + 2× nmol C_2H_4. [e] ND, not detectable.

increasing with molar ratios up to 20:1 and saturating above 30:1.

The dependence of the specific activities for N_2 and C_2H_2 reduction on their partial pressures is presented for both MoFe and FeFe in Figure 2. Fits of the data to a binding isotherm show that Fe-nitrogenase has a 4−5-fold higher apparent K_m (0.56 ± 0.06 atm) for N_2 than Mo-nitrogenase (0.13 ± 0.03 atm) and a 2.5-fold lower V_{max}. Carrying the fits out to high P_{N_2} shows that MoFe protein would asymptotically approach saturation for $P_{N_2} \gtrsim 50$ atm, consistent with the experimental study carried out to 50 atm.[32] Because of the higher apparent K_m for FeFe protein, an equivalent approach to saturation would require a far higher value, $P_{N_2} \gtrsim 210$ atm. For the reduction of acetylene, Fe-nitrogenase shows a 4-fold lower V_{max} and a ∼16-fold higher apparent K_m compared to those of Mo-nitrogenase (Figure 2). Specific activities and total electron flux at P_{N_2} = 1 atm and $P_{C_2H_2}$ = 0.3 atm are summarized in Table 1.

The effect of the partial pressure of N_2 and C_2H_2 on electron partitioning between N_2 or C_2H_2 reduction and proton reduction to make H_2 was examined (Figures 3 and 4). For Mo-nitrogenase, increasing P_{N_2} rapidly inhibits H^+ reduction, with ∼70% inhibition at 1 atm N_2. At this value of P_{N_2}, the ratio of H_2 formed to N_2 reduced is the product ratio $H_2/(NH_3/2) \sim 2$, about twice the limiting value of unity that is found at 50 atm and is associated with eq 1. For Fe-nitrogenase, the H_2 production in the absence of N_2 is about half that of Mo-nitrogenase and N_2 is about half as effective as an inhibitor of H_2 formation, decreasing it by ∼40% at P_{N_2} = 1 atm (Figure 3 and Table 1). However, because Fe-nitrogenase is significantly less active in reducing N_2, at P_{N_2} = 1 atm the ratio of H_2 formed per N_2 reduced is given by the product ratio, $H_2/N_2 \sim 7$, close to that reported previously and more than triple the value for Mo-nitrogenase at this N_2 pressure.

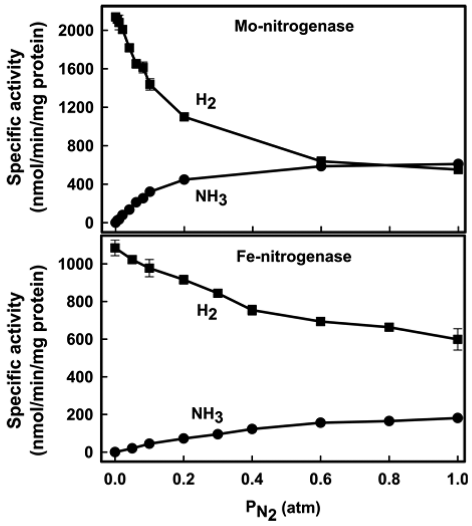

Figure 3. Effect of increasing partial pressure of N_2 (P_{N_2}) on N_2 (●) and H^+ (■) reduction in Mo-nitrogenase (top) and Fe-nitrogenase (bottom). Data points are connected with a solid line as a guide. Data are the average of two independent experiments with error bars. Assays were performed as described in Materials and Methods.

C_2H_2 is a good substrate and potent inhibitor of H^+ reduction in MoFe, essentially quenching all H_2 production by $P_{C_2H_2} \sim 0.2$ atm (Figure 4). In the case of FeFe protein, the inhibition is far weaker, with H_2 formation decreased by only

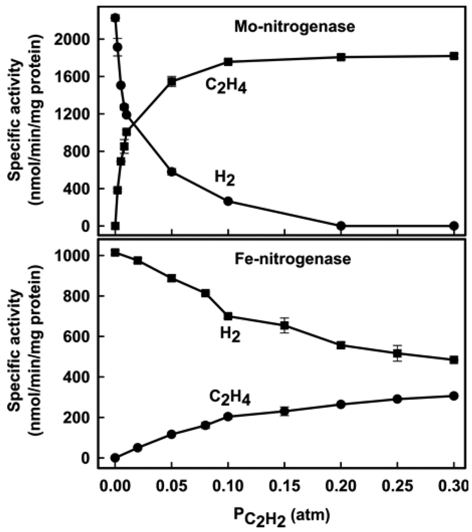

Figure 4. Effect of increasing partial pressure of acetylene ($P_{C_2H_2}$) on acetylene (●) and H^+ (■) reduction in Mo-nitrogenase (top) and Fe-nitrogenase (bottom). Data points are connected with a solid line as a guide. Data are the average of two independent experiments with error bars. Assays were performed as described in Materials and Methods.

about a factor of 2 at $P_{C_2H_2}$ = 0.3 atm, at which pressure more H_2 is still formed than C_2H_4 (Figure 4).

H_2 Inhibition of N_2 Reduction. The ability of H_2 to inhibit N_2 reduction was examined. For Mo-nitrogenase, when N_2 is held at 0.2 atm, increasing H_2 up to 0.8 atm suppresses of N_2 reduction by up to 70% compared to the no-H_2 condition. For Fe-nitrogenase, even though the activity is half that of MoFe in the absence of added H_2, a similar trend is observed. At 0.6 atm N_2, addition of H_2 up to 0.4 atm shows approximately 60% inhibition of N_2 reduction (Figure 5).

HD Formation. D_2 does not interact with nitrogenase in the absence of N_2. As a result, the most dramatic manifestation of the *re*/*oa* mechanism in Mo-nitrogenase is seen during reduction of N_2 in the presence of D_2. Under these conditions, D_2 *does* react, being stoichiometrically reduced to form 2HD formed per D_2 according to eq 2

$$D_2 + 2H^+(aq) + 2e^- \xrightarrow[\text{nitrogenase}]{N_2} 2HD \qquad (2)$$

This phenomenon is explained as arising through the *oa* of D_2 with release of N_2 and formation of two solvent nonexchangeable, bridging deuterides, [Fe—D—Fe], and then the sequential protonation of these D^- by H^+ from solvent (Figure 6).

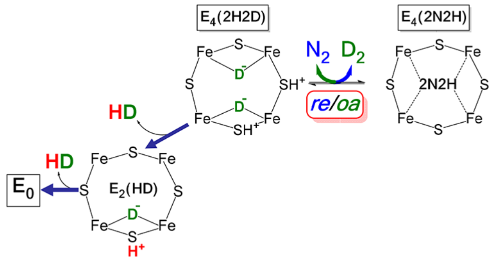

Figure 6. HD formation by nitrogenase. Shown is one FeS face of FeMo-cofactor with a reversible *re*/*oa* equilibrium for N_2 or D_2 binding. The pathway to the left leads to the formation of 2 equiv of HD. The deutrides (green) are not solvent exchangeable, whereas the protons (red) are solvent exchangeable.

To test for HD formation by Fe-nitrogenase, the enzyme was turned over under a range of partial pressures of N_2 and D_2, and the production of H_2 and HD was monitored by mass spectrometry. The volumes of H_2 produced, as measured in the headspace of the reaction vials, do not vary significantly up to a ratio of partial pressures N_2/D_2 = 0.7/0.3 (Figure 7, top). Upon further increase of this ratio, to a N_2/D_2 = 0.9/0.1 gas mixture, the volume of H_2 produced may begin to decrease, as might be expected from an increase in the proportion of the turnover electron flux going to N_2 reduction, leaving less for H_2 formation. However, the small magnitude of this effect, even at the N_2/D_2 = 0.9/0.1 pressure ratio, is consistent with literature reports and with our results for N_2 reduction presented above.

In testing for HD formation during N_2 reduction, it is important to note that HD is present in all samples, including no-turnover samples, because of HD contamination in the D_2 gas (Table S1). However, *every* FeFe protein turnover sample contained more HD than its paired no-turnover sample. This establishes that HD is produced by Fe-nitrogenase during N_2 turnover in the presence of D_2, an observation that by itself requires that Fe-nitrogenase carries out nitrogen fixation by the same *re*/*oa* mechanism as has been established for Mo-nitrogenase (Figure 6).

The amount of HD produced under various assay conditions was determined by subtraction of the HD background measured in the corresponding no-turnover samples. Figure 7, bottom, shows that the amount of HD produced during Fe-nitrogenase turnover exhibits a strong dependence on the ratio

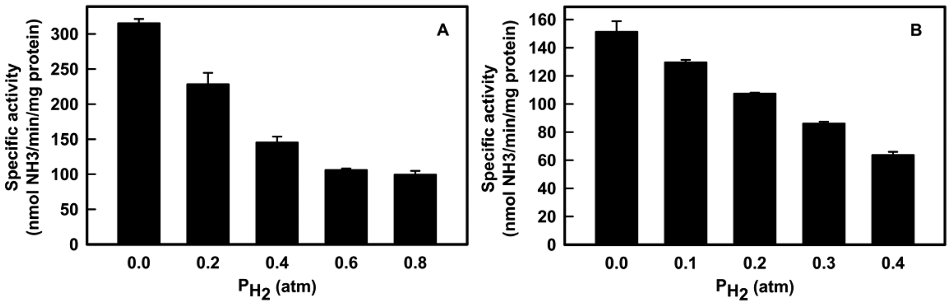

Figure 5. H_2 inhibition of N_2 reduction. Shown is the specific activity for N_2 reduction as a function of the partial pressure of H_2 for Mo-nitrogenase (A) and Fe-nitrogenase (B). Data are the average of two independent experiments with error bars. Assays were performed as described in Materials in Methods. For Mo-nitrogenase, N_2 was held at 0.2 atm and H_2 was varied. For Fe-nitrogenase, N_2 was held at 0.6 atm and H_2 was varied.

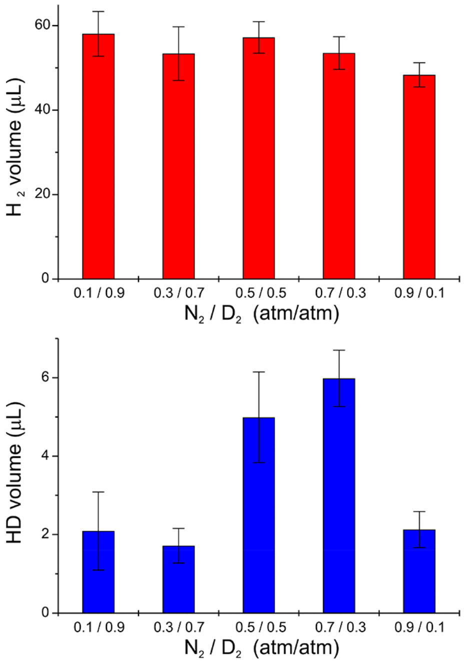

Figure 7. HD formation by Fe-nitrogenase. Volumes of produced H_2 (upper) and HD (lower) (1 atm, 295 K) in the headspace of turnover sample vials as a function of the ratio of N_2 and D_2 partial pressures (see Materials and Methods); error bars represent standard deviations.

of the pressures of N_2 and D_2 during reaction: The HD volume maximizes at ratios $N_2/D_2 \sim 1-2$ (0.5/0.5 and 0.7/0.3 atm) and is significantly lower at both higher and lower tested ratios, as revealed by statistical tests described in Materials and Methods. During turnover by Fe-nitrogenase and Mo-nitrogenase at the same Fe protein to MoFe protein/FeFe protein ratio, Fe-nitrogenase produces its maximum amount of HD, ~6 μL per 0.4 mg FeFe protein, at the ratio $N_2/D_2 \approx 0.7/0.3 \approx 2.3$, whereas the HD maximum of Mo-nitrogenase occurs at a ratio less than unity, $N_2/D_2 \approx 0.2/0.6 \approx 0.33$, where it produces roughly ~12-fold more HD per mol of protein, ~35 μL per 0.2 mg MoFe protein (Figure S4).

This dependence of HD formation by Fe-nitrogenase on the N_2/D_2 ratio (Figure 7, bottom) is explained by and reveals details of the *re*/*oa* mechanism. HD formation maximizes when the ratio of partial pressures is such that the N_2 partial pressure is high enough that the *re*/*oa* equilibrium significantly populates E_4(2N2H), $N_2/D_2 \sim 1-2$, but at the same time the partial pressure of D_2 is sufficiently high that D_2 can effectively react with this state through *oa* with the release of N_2 and formation of the HD-producing E_4(2H,2D) state (Figure 6). As the N_2 partial pressure is increased and D_2 decreased (e.g., N_2/D_2 = 0.9/0.1), the population of the E_4(2N2H) state increases, but because the partial pressure of D_2 is now small, so is the extent of D_2 *oa* by the E_4(2N2H) state to form the HD-producing dideuteride intermediate, E_4(2H,2D), and so HD production decreases.

At the other extreme of the N_2/D_2 ratio, when N_2 concentration is low and D_2 is high (e.g., N_2/D_2 = 0.1/0.9), the population of E_4(2N2H) is low, which precludes substantial *oa* of D_2 by E_4(2N2H) to form the E_4(2H,2D) state, despite the high D_2 partial pressure, and so HD production is low.

DISCUSSION

N_2 Reduction without Mo. The discovery of Mo-dependent nitrogenase was followed by the synthesis of mononuclear Mo-complexes that bound, activated, and ultimately reduced N_2.[44,45] Combined, these findings led to the assumption that Mo was necessary for N_2 reduction in nitrogenase. This assumption was later challenged by the demonstration of N_2 fixation by bacterial strains with deletions of the Mo-nitrogenase genes and cells grown in Mo-deficient media.[46−48] However, doubts about Mo-independent N_2 reduction remained until purified V- and Fe-nitrogenase[24,26,49−51] systems with very little Mo content were shown to be capable of N_2 fixation, solidifying that Mo was not essential for N_2 reduction in nitrogenase. As reported here, highly purified FeFe protein from *A. vinelandii* has Mo and V below the detection limit of our plasma emission method, placing the Mo and V content below 0.07 mol Mo or 0.005 mol V/mol FeFe protein. We find that the FeFe protein has an N_2 reduction specific activity of 181 nmol NH_3/min/mg FeFe protein compared to a value of 605 nmol NH_3/min/mg MoFe protein. The 3-fold lower N_2 reduction activity for the FeFe protein compared to the MoFe protein contrasts with the greater than 28-fold difference in Mo or V content (2 Mo per MoFe protein versus <0.07 Mo or <0.005 V per FeFe protein). Combined with the earlier work, these results clearly indicate that Mo and V are not required for nitrogenase N_2 reduction.

This conclusion is in line with other evidence pointing to the FeS portion of the nitrogenase active site providing the location of hydride accumulation and N_2 activation.[13] First, amino acid substitution studies near FeMo-cofactor pointed to one FeS face, the one that includes Fe atoms 2, 3, 6, 7 (numbering from the X-ray structure), as the site of N_2 binding.[42,52] Second, ^{95}Mo ENDOR showed that Mo is not an "anchoring" atom of the two metal-bridging hydrides of E_4(4H), which thus have the form [Fe−H−Fe].[53] Further, ENDOR/ESEEM spectroscopic studies of a catalytic intermediate of N_2 reduction by the MoFe protein enriched with ^{95}Mo showed no evidence for substrate binding or for oxidation state changes of the Mo.[13,19] The findings certainly implicate the FeS portion of the active site metal cluster in substrate reduction, but they do not exclude the involvement of Mo in some as yet untrapped state. In support of the reactivity of the Fe portion of FeMo-co are a number of recent studies on Fe-complexes that have been shown to activate and reduce N_2.[54,55] Taken together, these observations demonstrate that N_2 reduction can occur at Fe-based metal clusters, both outside and within nitrogenase proteins, and that many, if not all, of the stages of N_2 reduction by nitrogenase occur at Fe.

N_2 Reduction Mechanism. N_2 reduction by Mo-nitrogenase can be understood in terms of a reductive elimination mechanism whereby two bridging hydrides bound to Fe atoms of the E_4 state of FeMo-cofactor combine to generate H_2 and a doubly reduced FeMo-cofactor that is primed for N_2 binding and activation.[13] This mechanism explicitly incorporates, as a limiting stoichiometry of reaction, that eight electrons and protons are required and one H_2 is produced for each N_2 reduced, consistent with experiments at P_{N_2} = 50 atm.[32] However, the reaction stoichiometry observed for the Fe-nitrogenase, both in earlier work[9] and as reported here, clearly show that even at P_{N_2} = 1 atm, Fe-nitrogenase makes much more H_2 than Mo-nitrogenase, and the ratio of product formation is $H_2/N_2 \sim 6-7$, raising the question: does Fe-nitrogenase follow the same reductive elimination mechanism for N_2 activation?

This question is answered by an analysis of two properties of N_2 reduction catalyzed by nitrogenase: (i) the ability of H_2 to inhibit N_2 reduction and (ii) the ability of nitrogenase to catalyze the formation of HD when run under N_2 and D_2. H_2 inhibition of N_2 reduction by nitrogenase was reported in some of the earliest kinetic studies of nitrogenase.[56] This inhibition can be understood in terms of the reversibility of the N_2 binding/H_2 release step in the reductive elimination/oxidative addition mechanism (Figure 1C). Excess H_2 reverses the E_4 *re/oa* equilibrium to the left, in effect introducing a nonproductive reaction pathway, lowering the occupancy of the N_2 bound state and net N_2 reduction activity, and enhancing the return to the resting state with loss of two H_2. This *re/oa* equilibrium has been validated by spectroscopic quantification of trapped states under different N_2 and H_2 concentrations.[16−18] As can be seen in Figure 5, Fe-nitrogenase shows a similar pattern of H_2 inhibition of N_2 reduction to that observed in Mo-nitrogenase, although at different concentrations of N_2 and H_2. This parallelism in H_2 inhibition of N_2 reduction between the two nitrogenases suggests that they share a similar mechanism (Figure 1C).

The formation of HD when nitrogenase is turned over under a mixture of N_2 and D_2 is, however, the definitive test for a reversible *re/oa* mechanism at E_4 in nitrogenase.[20] No explanation had been offered for the fact that whereas Mo-nitrogenase does not react with H_2/D_2 at all in the absence of N_2, the enzyme nonetheless acts as catalyst for the stoichiometric reduction of D_2 to 2HD, with N_2 as a cocatalyst, eq 2, until it was recognized that the *re/oa* equilibrium explains this reaction as shown in Figure 6.[13] The present experiments clearly show that, as is observed for Mo-nitrogenase, Fe-nitrogenase likewise catalyzes the reduction of D_2 to HD dependent on the presence of N_2 (Figure 7). Thus, based on the observations of H_2 inhibition and HD formation, the conclusion is inescapable that both Mo- and Fe-nitrogenase utilize a similar *re/oa* mechanism for N_2 reduction.

Measurements presented above offer an explanation for why the observed product ratio, H_2-formed/N_2-reduced, at $P_{N_2} = 1$ atm is so much greater for Fe-nitrogenase than for Mo nitrogenase: H_2/N_2 ~7 versus ~2. The activity measurements actually show that Fe-nitrogenase is 2-fold less active at proton reduction in the absence of N_2 than Mo-nitrogenase (e.g., Fe-nitrogenase has an overall lower electron flux). They also show that Fe-nitrogenase has a rather similarly decreased effectiveness for N_2 reduction, having a V_{max} for N_2 reduction ~2.5-fold smaller than that for Mo-nitrogenase. Thus, the replacement of Fe for Mo and the different protein environments of the two proteins decrease the effectiveness of both H^+ reduction to H_2 and of N_2 reduction by roughly similar amounts in Fe-nitrogenase, and therefore these changes cannot account for the high value of the H_2/N_2 ratio for Fe-nitrogenase. Instead, the significant difference between the two enzymes is that they differ sharply in the K_m for N_2, which is 5-fold higher for Fe-nitrogenase than for Mo-nitrogenase. In short, it appears that the greater production of H_2 by Fe-nitrogenase under 1 atm of N_2 is largely because the N_2 pressures used to date (1 atm or less) are insufficient for N_2 reduction to suppress/outcompete hydride protonation to form H_2.

The differences between the reactivity at FeMo-co and FeFe-co surely reflect the presence of Mo versus Fe, but it can be influenced by the differences in the protein surrounding each cofactor. A homology model for the protein environment predicted around FeFe-co has been reported, showing many similarities to the MoFe protein environment around FeMo-co, as well as some key alterations in amino acids.[30] Analysis of the influence of these protein changes on reactivity will require additional experimental and theoretical studies. Given the recent observation of carbonate instead of a sulfur in the VFe-cofactor,[15] it is possible that such a variation in ligands may also be found in the FeFe-cofactor, influencing reactivity. Deducing the relative roles of these factors in controlling the reactivity of Mo- and Fe-nitrogenase will provide valuable insights into how these enzymes meet the challenge of N_2 reduction, but ultimately, as shown here, they both utilize the same fundamental mechanism for N_2 binding and activation.

■ ASSOCIATED CONTENT

Supporting Information

The Supporting Information is available free of charge on the ACS Publications website at DOI: 10.1021/acs.biochem.7b01142.

> Examples of $m/z = 2$ and 3 signals for FeFe samples prepared at $N_2/D_2 = 0.5/0.5$ and 0.9/0.1; Coomassie stained SDS-PAGE gel of purified FeFe protein along with densitometry data; dependence of HD contamination in "no-turnover" samples on P_{D_2}; protein identification within Fe-nitrogenase complex purified from *A. vinelandii*; comparison of HD production by MoFe and FeFe nitrogenases at their optimal assay conditions (PDF)

■ AUTHOR INFORMATION

Corresponding Authors

*E-mail: bmh@northwestern.edu. Phone: +1-847-491-3104 (B.M.H.).
*E-mail: lance.seefeldt@usu.edu. Phone: +1-435-797-3964 (L.C.S.).

ORCID

Derek F. Harris: 0000-0003-4277-2976
Neil Kelleher: 0000-0002-8815-3372
Brian M. Hoffman: 0000-0002-3100-0746
Lance C. Seefeldt: 0000-0002-6457-9504

Funding

Support for the cell growth, protein purification, and kinetic analysis was provided by the U.S. Department of Energy, Office of Science, Basic Energy Sciences (BES) under awards to L.C.S. and D.R.D. (DE-SC0010687 and DE-SC0010834). Support for HD exchange measurements was provided by a grant from the National Institutes of Health to B.M.H. (GM111097). Protein mass spectrometry work was done as part of the Biological Electron Transfer and Catalysis (BETCy) Energy Frontiers Research Center (EFRC) supported by the Department of Energy (DE-SC0012518). The Mass Spectrometry Facility at MSU is supported in part by the Murdock Charitable Trust and an NIH IDEA program grant P20GM103474.

Notes

The authors declare no competing financial interest.
Data sets in comma delimited format for Figures 2−5 are available at DOI: 10.5281/zenodo.1040952.

■ ACKNOWLEDGMENTS

The authors thank Carrie Harwood, Katie Fixen, and Yanning Zheng for discussions on Fe only nitrogenase.

■ REFERENCES

(1) Raymond, J., Siefert, J. L., Staples, C. R., and Blankenship, R. E. (2004) The natural history of nitrogen fixation. *Mol. Biol. Evol. 21*, 541−554.

(2) Burris, R. H., and Roberts, G. P. (1993) Biological nitrogen fixation. *Annu. Rev. Nutr. 13*, 317−35.

(3) Gruber, N., and Galloway, J. N. (2008) An Earth-system perspective of the global nitrogen cycle. *Nature 451*, 293−296.

(4) Eady, R. R. (1996) Structure-function relationships of alternative nitrogenases. *Chem. Rev. 96*, 3013−3030.

(5) Burgess, B. K., and Lowe, D. J. (1996) Mechanism of molybdenum nitrogenase. *Chem. Rev. 96*, 2983−3012.

(6) Hu, Y., Lee, C. C., and Ribbe, M. W. (2012) Vanadium nitrogenase: A two-hit wonder? *Dalton Trans. 41*, 1118−1127.

(7) Robson, R., Woodley, P., and Jones, R. (1986) Second gene (nifH*) coding for a nitrogenase iron protein in *Azotobacter chroococcum* is adjacent to a gene coding for a ferredoxin-like protein. *EMBO J. 5*, 1159−1163.

(8) Joerger, R. D., Jacobson, M. R., Premakumar, R., Wolfinger, E. D., and Bishop, P. E. (1989) Nucleotide sequence and mutational analysis of the structural genes (anfHDGK) for the second alternative nitrogenase from *Azotobacter vinelandii*. *J. Bacteriol. 171*, 1075−1086.

(9) Schneider, K., and Müller, A. (2004) Iron-only nitrogenase: Exceptional catalytic, structural and spectroscopic features, in *Catalysts for Nitrogen Fixation*, pp 281−307, Springer, Dordrecht.

(10) Fay, A. W., Blank, M. A., Lee, C. C., Hu, Y., Hodgson, K. O., Hedman, B., and Ribbe, M. W. (2010) Characterization of isolated nitrogenase FeVco. *J. Am. Chem. Soc. 132*, 12612−12618.

(11) Krahn, E., Weiss, B., Kröckel, M., Groppe, J., Henkel, G., Cramer, S., Trautwein, A., Schneider, K., and Müller, A. (2002) The Fe-only nitrogenase from *Rhodobacter capsulatus*: identification of the cofactor, an unusual, high-nuclearity iron-sulfur cluster, by Fe K-edge EXAFS and ^{57}Fe Mössbauer spectroscopy. *JBIC, J. Biol. Inorg. Chem. 7*, 37−45.

(12) Hales, B. J. (1990) Alternative nitrogenase. *Adv. Inorg. Biochem. 8*, 165−198.

(13) Hoffman, B. M., Lukoyanov, D., Yang, Z.-Y., Dean, D. R., and Seefeldt, L. C. (2014) Mechanism of nitrogen fixation by nitrogenase: The next stage. *Chem. Rev. 114*, 4041−4062.

(14) Howard, J. B., and Rees, D. C. (2006) How many metals does it take to fix N_2? A mechanistic overview of biological nitrogen fixation. *Proc. Natl. Acad. Sci. U. S. A. 103*, 17088−17093.

(15) Sippel, D., and Einsle, O. (2017) The structure of vanadium nitrogenase reveals an unusual bridging ligand. *Nat. Chem. Biol. 13*, 956−960.

(16) Lukoyanov, D., Khadka, N., Yang, Z.-Y., Dean, D. R., Seefeldt, L. C., and Hoffman, B. M. (2016) Reversible photoinduced reductive elimination of H_2 from the nitrogenase dihydride state, the E4(4H) Janus intermediate. *J. Am. Chem. Soc. 138*, 1320−1327.

(17) Lukoyanov, D., Khadka, N., Yang, Z.-Y., Dean, D. R., Seefeldt, L. C., and Hoffman, B. M. (2016) Reductive elimination of H_2 activates nitrogenase to reduce the N≡N triple bond: characterization of the E4(4H) Janus intermediate in wild-type enzyme. *J. Am. Chem. Soc. 138*, 10674−10683.

(18) Lukoyanov, D., Yang, Z.-Y., Khadka, N., Dean, D. R., Seefeldt, L. C., and Hoffman, B. M. (2015) Identification of a key catalytic intermediate demonstrates that nitrogenase is activated by the reversible exchange of N_2 for H_2. *J. Am. Chem. Soc. 137*, 3610−3615.

(19) Lukoyanov, D., Yang, Z.-Y., Barney, B. M., Dean, D. R., Seefeldt, L. C., and Hoffman, B. M. (2012) Unification of reaction pathway and kinetic scheme for N_2 reduction catalyzed by nitrogenase. *Proc. Natl. Acad. Sci. U. S. A. 109*, 5583−5587.

(20) Burgess, B. K., Wherland, S., Newton, W. E., and Stiefel, E. I. (1981) Nitrogenase reactivity: insight into the nitrogen-fixing process through hydrogen-inhibition and HD-forming reactions. *Biochemistry 20*, 5140−5146.

(21) Guth, J. H., and Burris, R. H. (1983) Inhibition of nitrogenase-catalyzed ammonia formation by hydrogen. *Biochemistry 22*, 5111−5122.

(22) Lee, C. C., Hu, Y., and Ribbe, M. W. (2009) Unique features of the nitrogenase VFe protein from *Azotobacter vinelandii*. *Proc. Natl. Acad. Sci. U. S. A. 106*, 9209−9214.

(23) Pau, R. N., Eldridge, M. E., Lowe, D. J., Mitchenall, L. A., and Eady, R. R. (1993) Molybdenum-independent nitrogenases of *Azotobacter vinelandii*: a functional species of alternative nitrogenase-3 isolated from a molybdenum-tolerant strain contains an iron-molybdenum cofactor. *Biochem. J. 293*, 101−107.

(24) Chisnell, J. R., Premakumar, R., and Bishop, P. E. (1988) Purification of a second alternative nitrogenase from a nifHDK deletion strain of *Azotobacter vinelandii*. *J. Bacteriol. 170*, 27−33.

(25) Schneider, K., Gollan, U., Dröttboom, M., Selsemeier-Voigt, S., and Müller, A. (1997) Comparative biochemical characterization of the iron-only nitrogenase and the molybdenum nitrogenase from *Rhodobacter capsulatus*. *Eur. J. Biochem. 244*, 789−800.

(26) Schneider, K., Müller, A., Schramm, U., and Klipp, W. (1991) Demonstration of a molybdenum-and vanadium-independent nitrogenase in a nifHDK-deletion mutant of *Rhodobacter capsulatus*. *Eur. J. Biochem. 195*, 653−661.

(27) Müller, A., Schneider, K., Knüttel, K., and Hagen, W. R. (1992) EPR spectroscopic characterization of an ‘iron only nitrogenase S= 3/2 spectrum of component 1 isolated from *Rhodobacter capsulatus*. *FEBS Lett. 303*, 36−40.

(28) Davis, R., Lehman, L., Petrovich, R., Shah, V. K., Roberts, G. P., and Ludden, P. W. (1996) Purification and characterization of the alternative nitrogenase from the photosynthetic bacterium *Rhodospirillum rubrum*. *J. Bacteriol. 178*, 1445−1450.

(29) Schüddekopf, K., Hennecke, S., Liese, U., Kutsche, M., and Klipp, W. (1993) Characterization of anf genes specific for the alternative nitrogenase and identification of nif genes required for both nitrogenases in *Rhodobacter capsulatus*. *Mol. Microbiol. 8*, 673−684.

(30) Mcglynn, S. E., Boyd, E. S., Peters, J. W., and Orphan, V. J. (2013) Classifying the metal dependence of uncharacterized nitrogenases. *Front. Microbiol. 3*, 419.

(31) Thorneley, R. N. F., and Lowe, D. J. (1985) Kinetics and mechanism of the nitrogenase enzyme, in *Molybdenum Enzymes* (Spiro, T. G., Ed.), pp 221−284, Wiley-Interscience Publications, New York.

(32) Simpson, F. B., and Burris, R. H. (1984) A nitrogen pressure of 50 atm does not prevent evolution of hydrogen by nitrogenase. *Science 224*, 1095−1097.

(33) Robinson, A. C., Burgess, B. K., and Dean, D. R. (1986) Activity, reconstitution, and accumulation of nitrogenase components in Azotobacter vinelandii mutant strains containing defined deletions within the nitrogenase structural gene cluster. *J. Bacteriol. 166*, 180−186.

(34) Toukdarian, A., and Kennedy, C. (1986) Regulation of nitrogen metabolism in *Azotobacter vinelandii*: isolation of ntr and glnA genes and construction of ntr mutants. *EMBO J. 5*, 399−407.

(35) Christiansen, J., Goodwin, P. J., Lanzilotta, W. N., Seefeldt, L. C., and Dean, D. R. (1998) Catalytic and biophysical properties of a nitrogenase apo-MoFe protein produced by an nifB-deletion mutant of *Azotobacter vinelandii*. *Biochemistry 37*, 12611−12623.

(36) Burgess, B. K., Jacobs, D. B., and Stiefel, E. I. (1980) Large-scale purification of high activity *Azotobacter vinelandii* nitrogenase. *Biochim. Biophys. Acta 614*, 196−209.

(37) Peters, J. W., Fisher, K., and Dean, D. R. (1994) Identification of a nitrogenase protein-protein interaction site defined by residues 59 through 67 within the *Azotobacter vinelandii* Fe protein. *J. Biol. Chem. 269*, 28076−28083.

(38) Yang, Z.-Y., Ledbetter, R., Shaw, S., Pence, N., Tokmina-Lukaszewska, M., Eilers, B., Guo, Q., Pokhrel, N., Cash, V. L., Dean, D. R., Antony, E., Bothner, B., Peters, J. W., and Seefeldt, L. C. (2016)

Evidence that the P_i release event is the rate-limiting step in the nitrogenase catalytic cycle. *Biochemistry 55,* 3625−3635.

(39) Vaudel, M., Burkhart, J. M., Zahedi, R. P., Oveland, E., Berven, F. S., Sickmann, A., Martens, L., and Barsnes, H. (2015) PeptideShaker enables reanalysis of MS-derived proteomics data sets. *Nat. Biotechnol. 33,* 22−24.

(40) Kelley, L. A., Mezulis, S., Yates, C. M., Wass, M. N., and Sternberg, M. J. E. (2015) The Phyre2 web portal for protein modeling, prediction and analysis. *Nat. Protoc. 10,* 845−858.

(41) Corbin, J. L. (1984) Liquid chromatographic-fluorescence determination of ammonia from nitrogenase reactions: A 2-min assay. *Appl. Environ. Microbiol. 47,* 1027−1030.

(42) Barney, B. M., Igarashi, R. Y., Dos Santos, P. C., Dean, D. R., and Seefeldt, L. C. (2004) Substrate interaction at an iron-sulfur face of the FeMo-cofactor during nitrogenase catalysis. *J. Biol. Chem. 279,* 53621−53624.

(43) Setubal, J. C., dos Santos, P., Goldman, B. S., Ertesvåg, H., Espin, G., Rubio, L. M., Valla, S., Almeida, N. F., Balasubramanian, D., Cromes, L., Curatti, L., Du, Z., Godsy, E., Goodner, B., Hellner-Burris, K., Hernandez, J. A., Houmiel, K., Imperial, J., Kennedy, C., Larson, T. J., Latreille, P., Ligon, L. S., Lu, J., Mærk, M., Miller, N. M., Norton, S., O'Carroll, I. P., Paulsen, I., Raulfs, E. C., Roemer, R., Rosser, J., Segura, D., Slater, S., Stricklin, S. L., Studholme, D. J., Sun, J., Viana, C. J., Wallin, E., Wang, B., Wheeler, C., Zhu, H., Dean, D. R., Dixon, R., and Wood, D. (2009) Genome sequence of *Azotobacter vinelandii,* an obligate aerobe specialized to support diverse anaerobic metabolic processes. *J. Bacteriol. 191,* 4534−4545.

(44) Yandulov, D. V., and Schrock, R. R. (2003) Catalytic reduction of dinitrogen to ammonia at a single molybdenum center. *Science 301,* 76−78.

(45) Pickett, C. J. (1996) The Chatt cycle and the mechanism of enzymic reduction of molecular nitrogen. *JBIC, J. Biol. Inorg. Chem. 1,* 601−606.

(46) Bishop, P. E., Jarlenski, D. M., and Hetherington, D. R. (1980) Evidence for an alternative nitrogen fixation system in *Azotobacter vinelandii. Proc. Natl. Acad. Sci. U. S. A. 77,* 7342−7346.

(47) Bishop, P. E., Premakumar, R., Dean, D. R., Jacobson, M. R., Chisnell, J. R., Rizzo, T. M., and Kopczynski, J. (1986) Nitrogen fixation by *Azotobacter vinelandii* strains having deletions in structural genes for nitrogenase. *Science 232,* 92−94.

(48) Bishop, P. E., Hawkins, M. E., and Eady, R. R. (1986) Nitrogen fixation in molybdenum-deficient continuous culture by a strain of *Azotobacter vinelandii* carrying a deletion of the structural genes for nitrogenase (nifHDK). *Biochem. J. 238,* 437−442.

(49) Eady, R. R., Robson, R. L., Richardson, T. H., Miller, R. W., and Hawkins, M. (1987) The vanadium nitrogenase of *Azotobacter chroococcum*. Purification and properties of the VFe protein. *Biochem. J. 244,* 197−207.

(50) Hales, B. J., Case, E. E., Morningstar, J. E., Dzeda, M. F., and Mauterer, L. A. (1986) Isolation of a new vanadium-containing nitrogenase from *Azotobacter vinelandii*. *Biochemistry 25,* 7251−7255.

(51) Müller, A., Schneider, K., Gollan, U., Krahn, E., and Dröttboom, M. (1995) Characterization of the "iron only" nitrogenase from *Rhodobacter capsulatus. J. Inorg. Biochem. 59,* 551−551.

(52) Dos Santos, P. C., Igarashi, R. Y., Lee, H.-I., Hoffman, B. M., Seefeldt, L. C., and Dean, D. R. (2005) Substrate interactions with the nitrogenase active site. *Acc. Chem. Res. 38,* 208−214.

(53) Lukoyanov, D., Yang, Z.-Y., Dean, D. R., Seefeldt, L. C., and Hoffman, B. M. (2010) Is Mo involved in hydride binding by the four-electron reduced (E4) intermediate of the nitrogenase MoFe protein? *J. Am. Chem. Soc. 132,* 2526−2527.

(54) Čorić, I., Mercado, B. Q., Bill, E., Vinyard, D. J., and Holland, P. L. (2015) Binding of dinitrogen to an iron-sulfur-carbon site. *Nature 526,* 96−99.

(55) Anderson, J. S., Rittle, J., and Peters, J. C. (2013) Catalytic conversion of nitrogen to ammonia by an iron model complex. *Nature 501,* 84−87.

(56) Rivera-Ortiz, J. M., and Burris, R. H. (1975) Interactions among substrates and inhibitors of nitrogenase. *J. Bacteriol. 123,* 537−545.